Low-temperature transition in non-centrosymmetric CoGe: the influence of the quadrupole transition on the occurrence of an incommensurate phase

A.V. Tsvyashchenko[1], V.A. Sidorov[1], A.V. Nikolaev[2], Seung-Ho Baek[3], T. Klimczuk[4], F. Ronning[5]

[1]Vereshchagin Institute of High Pressure Physics, RAS, Moscow, 108840, Russia
[2]Skobeltsyn Institute of Nuclear Physics Lomonosov Moscow State University, 119991 Moscow, Russia
[3]Changwon National University, 20 Changwondae-ro Uichang-gu Changwon-si, Gyeongsangnam-do 51140 Republic of Korea
[4]Faculty of Applied Physics and Mathematics, Gdansk University of Technology, Narutowicza 11/12, 80-233 Gdansk, Poland
[5]Los Alamos National Laboratory, MPA-CMMS, Los Alamos, New Mexico 87545, USA

tsvyash@hppi.troitsk.ru

MOTIVATION

Monogermanides like MnGe, FeGe, CoGe , RhGe and their monosilicides counterparts (MnSi, FeSi, CoSi, RhSi) with the B20 (T^4 or $P2_13$) crystal structure continue to attract much attention because of their remarkable electron and magnetic properties, including such topics as helimagnetism, quantum phase transition under hydrostatic pressure, associated with non non-Fermi liquid behavior, topological Hall effect, field-induced skyrmion lattices, long-wavelength *gapless* spin fluctuations (*phasons*), chiral topological fermions (*Dirac and Weyl fermions*) and the coexistence of superconductivity and magnetism. Formally the B20 structure is cubic, but in contrast to other proper cubic lattices (like *Fm3m* etc.), the cubic character of B20 is elusive. There are no cubes composed of B20 lattice sites, and with only four atoms of a 3d transition element and four atoms of germanium (or silicon) in its unit cell, the $P2_13$ group implies a very low local symmetry around each atom. In "true" cubic lattice sites the expansion of electron density in terms of spherical harmonics include contributions with (L = 0, 4, 6, ...) for cubic sites, and (L = 0, 3, 4, ...) for the tetrahedral lattice site. For the B20 crystal sites the tetrahedron composed of four nearest neighbors is not regular and has only one free fold rotational axis of symmetry along one of the four cube diagonals i.e. ($\pm1,\pm1,\pm1$). The lack of inversion symmetry gives rise to a mixture of even (L = 0, 2, ...) and odd (L = 1, 3, ...) components of the corresponding electron density. This results in anisotropic exchange interactions and the appearance of the Dzyaloshinskii-Moriya spin coupling, which can induce a spin-spiral wave propagation at low temperatures. Indeed, the helimagnetic ground state has been found in MnSi, FeGe and $Fe_{1-x}Co_xSi$.

Another remarkable feature of the *T*Si and *T*Ge compounds (*T* = Cr, Mn, Fe, Co) which differ mainly in the number of occupied electron 3d states, is a drastic change of their ground states. CrSi is a paramagnetic metal, MnSi is helimagnetic below 29 K, FeSi is a strongly correlated semiconductor with unusual temperature dependent properties. CoSi is three-dimensional (3D) topological Weyl semimetals (TWSs) in which is observed of unconventional chiral fermions with long Fermi arcs.

Unlike stable B20 phases of monosilicides, crystallization of *T*Ge in the B20 structure is conditional. The only metallic germanide having the equilibrium lattice of the B20 type is CrGe. By carefully controlling growth conditions, the B20 phase of FeGe can be readily obtained, while B20 phases of MnGe, CoGe and RhGe are metastable requiring high pressure and temperature for their synthesis.

Whereas CrGe is a simple paramagnetic metal, MnGe is a metal with complex magnetic behavior and two magnetic phase transitions (at 32 K and 175 K). Unlike insulating FeSi, FeGe displays a metallic and helimagnetic ground state. Finally, CoGe is a semimetal and the magnetic susceptibility.

measurements showed that CoGe is a Pauli paramagnet. Specific heat measurements of indicate that the electron specific heat coefficient γ is very close to zero, with a zero density of electron states (DOS) $N(E_F)$ at the Fermi energy. In however, a non-zero value of γ has been reported, $\gamma \approx 4$ mJ/mole K^2 [$N(E_F) \approx 1.6$ st/eV]. The density functional theory (DFT) calculations yield a small Fermi surface for CoGe with $N(E_F) \approx 4$ st/eV. Although the calculated density of states at E_F is at a minimum of the DOS curve, no energy gap around E_F has been found. Another characteristic feature of the band structure of CoGe is the Dirac cone with a flat band at the Γ point of the Brillouin zone near E_F, which possibly accounts for its large thermopower. Consistent with a small value of $N(E_F)$, the magnetic susceptibility χ of CoGe is very weak, and depending on the applied magnetic field H can be positive or negative. In high applied magnetic fields ($H >$ 15 kOe) χ is weakly diamagnetic, but becomes paramagnetic in small H. In small magnetic fields $\chi \sim 5\times10{-}6$ emu/g with a low temperature upturn due to a tiny amount of Co magnetic impurities. In contrast to FeGe, no antiferromagnetic transition in CoGe has been found. Depending on temperature, the carrier density of CoGe estimated from the high-field Hall effect ranges from 0.6 to 1.3 $\times$ 10^{21} cm^{-3} which results in about 0.04 charge carriers per CoGe formula unit. Despite the progress in understanding the electron and magnetic properties of CoGe, studies performed so far have overlooked a remarkable narrow peak at 13.4 - 14.0 K in the specific heat of CoGe. This peak and other anomalous behavior at temperatures below 30 K lead to a new physics, which is a subject of the present paper.

In all transition elements T under consideration the 3d electron shell is only partially occupied. This implies that the density matrix elements $\langle\psi_{lm}|\rho_{L,M}|\psi_{lm}\rangle$ for *d*-functions $l = l' = 2$ has a significant quadrupolar (L = 2) component at corresponding crystal sites. Quadrupolar contributions arise also from the mixture of 3*d* and 4*s* functions, characterized by the density matrix elements $\langle\psi_{lm}|\rho_{L,M}|\varphi_{l'=0}\rangle$, where the function $\varphi_{l'=0}$ refers to the 4*s* states. The appreciable quadrupolar density (L = 2) leads to strong anisotropic electronic interactions which can drive a structural or magnetic phase 2 transition.

Such a situation is not uncommon for 4*f*-elements, where a small quadrupole moment is caused by mixing of 4f-states. A well known example is CeB_6 (with the quadrupole transition occurs at the temperature T_Q = 3.3 K). Experimental aspects of quadrupolar order in TmCu, $PrPb_3$, TbP, DySb, $ErAl_2$, $TmGa_3$, CeMg, CeZn and related phenomena are discussed in reviews. Antiferro-quadrupolar ordering was found in TmTe (T_Q = 1.8 K) and NpO_2 (T_Q = 25.5 K). Quadrupole transitions were observed in UPd_3 and in the RB_2C_2 series (where R = Dy, Ho, Tb). As temperature decreases below T_Q = 24.7 K the superlattice peaks (h/2, k/2, 9/2) of reciprocal lattice develop in DyB_2C_2 and the (1, 0, 3) reflection in UPd_3.

Note that the appearance of superlattice peaks in all these compounds is in fact an indication of a crystal symmetry lowering. Therefore, the quadrupolar ordering is just a low temperature phase transition.

A change in structure and symmetry of the local environment of magnetic atom (with an open electron shell) can result in magnetic effects and magnetic ordering. Indeed the quadrupole phase transition is very often followed by magnetic ordering at a lower temperature $T_M < T_Q$. A clear cut illustration of this observation is the fullerene compound TDAE-C60 (this is the only organic compound displaying magnetic order below 16 K).

C60 two stable phases α and α' were found differing by the orientation of the C60 fullerene molecule. While the α phase is ferromagnetic with the critical temperature T_M = 16 K, its counterpart α' is found nonmagnetic.

For the B20 structure the connection between crystalline chirality and chirality of a helical magnetic structure was reported and discussed by Grigoriev et al. for Fe-doped MnSi.

Quadrupolar phase transitions can occur in 3d based compounds as well. In respect to the B20 structure it requires a change of orientation and the value of quadrupoles composed of the 3*d* and 4*s* electron states. However, unlike other phase transitions to commensurate phases, the lowering of space symmetry in CoGe leads to incommensurate (modulated) phase at low temperatures. In the present study we will show that the transition to incommensurate structure can account for low temperature anomalous behavior of CoGe.

EXPERIMENT AND THEORY

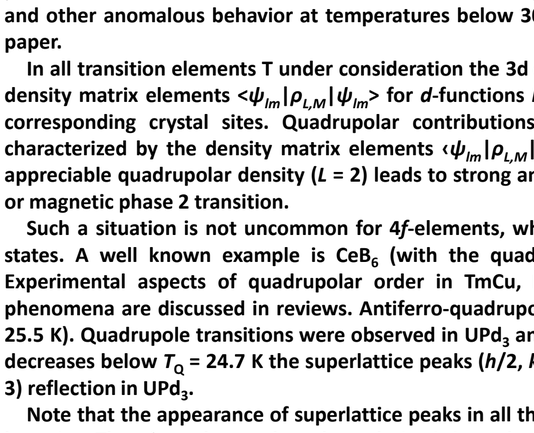

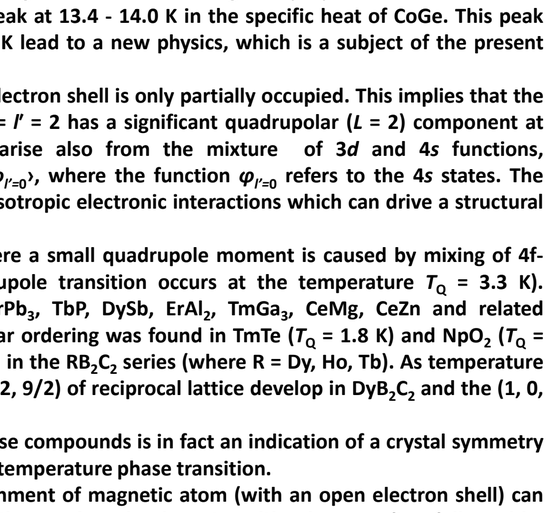

Fig. 1. X-ray powder diffraction pattern of CoGe (B20) measured at T = 295 K, P = 0 GPa

Fig.2 The specific heat of CoGe (in the form *C/T*) between 2 K and 300 K. The insert show the behavior of the specific heat around the transition in magnetic fields up to 9 T.

Where the nuclear magnetization is as follows:

$$M(2\tau) = M_0 \exp\left(-\frac{2\tau}{T_{2L}}\right) \exp\left(-\frac{1}{2}\left(\frac{2\tau}{T_{2G}}\right)^2\right)$$

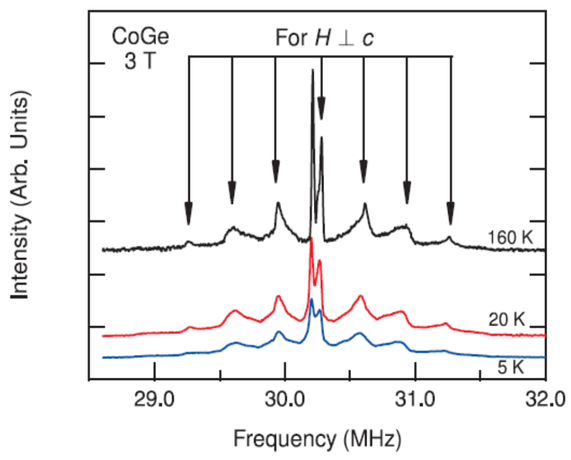

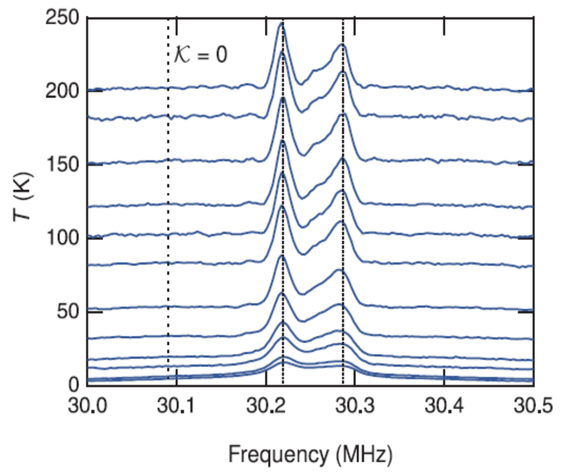

Fig. 3. A typical spectral pattern in a powder observed for I = 7/2 nuclei in an axial symmetry — the quadrupole frequency ω_Q = 0.67 MHz which is independent of temperature

Fig. 4. The T dependence of the central line : the whole spectrum does not shift with temperature

The Knight shift for any direction of magnetic field is *T*-independent.

The line clearly broadens below ~30 K. One could see the noticeable broadening in the full spectrum shown above. This is ascribed to short-range spin correlations.

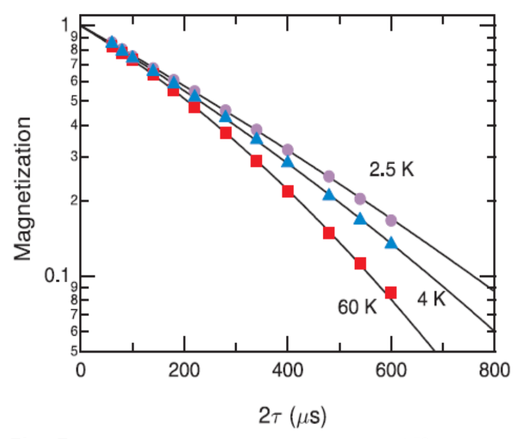

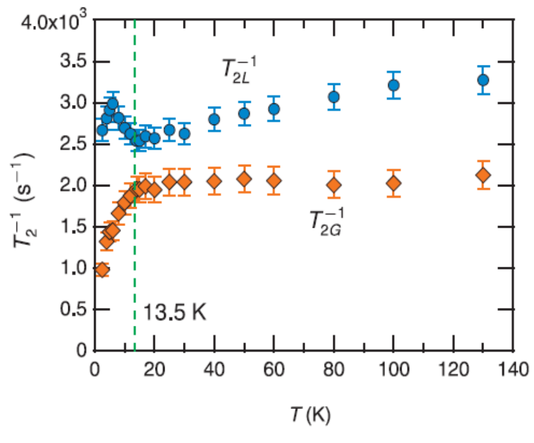

Fig. 5. The nuclear magnetization M of ^{59}Co is described by both the Lorentzian and Gaussian relaxation rate, $1/T_{2L}$ and $1/T_{2G}$.

Fig. 6. Temperature dependence of the relaxation rates of $^{-}T^{1}_{2L}$ and T^{-1}_{2G}

Clearly, both T_{2L} and T_{2G} change abruptly at 13.5 K. Below the transition, the Gaussian contribution gets progressively weaker and the Lorentzian term which is associated with the spin-lattice relaxation process becomes dominant. (Note that the temperature dependence of $1/T_{2L}$ is similar to that of $1/T_1$)

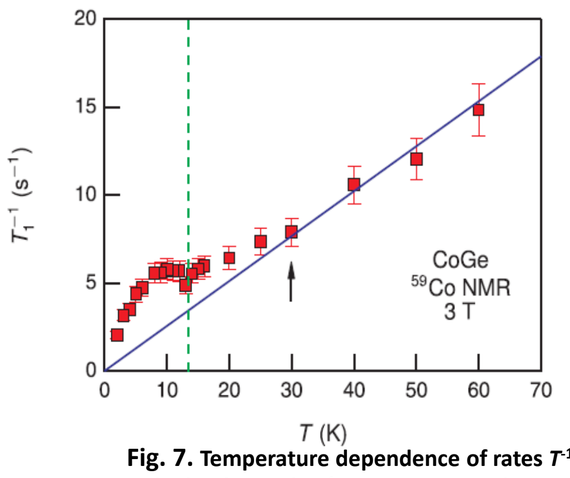

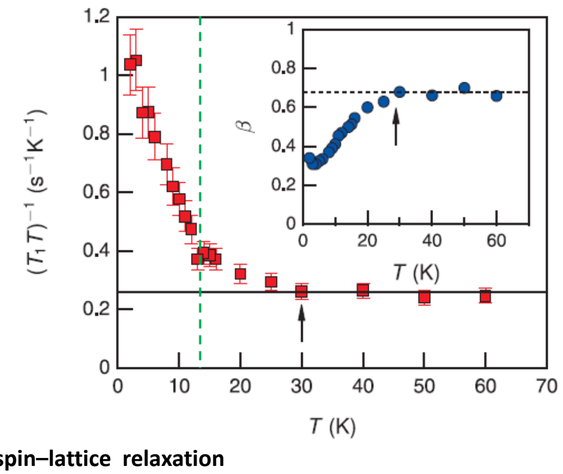

Fig. 7. Temperature dependence of rates T^{-1}_1 of spin–lattice relaxation

At high T (> 30 K), $1/T_1$ is proportional to T, as in a metal. (This is consistent with the constant Knight shift, i.e., the Korringa behavior) Below 30 K, it deviates from the linear T dependence, and shows an anomalous change at 13.5 K.

Fig. 8. Temperature dependence of $1/T_1T$

$1/T_1T$ reveals two characteristic temperatures.

(1) At 30 K, $1/T_1T$ starts to increase. At the same time, the stretching exponent β is rapidly reduced from a constant, indicating that $1/T_1$ gets strongly spatially distributed, i.e., the system becomes magnetically inhomogeneous. This accounts for the inhomogeneous line broadening below 30 K. 30 K appears to be the onset of short-range spin correlations.

(2) At 13.5 K, $1/T_1T$ shows a clear kink which is consistent with the anomaly observed in $1/T_2$ vs T. Interestingly, the Knight shift does not show any anomaly at all measured temperatures. That is, the transition at 13.5 K causes the change of spin dynamics without involving static spin order.

CONCLUSIONS

The group theoretical analysis shows that there is only one relatively high symmetry for the quadrupole ordering, which is the *R3* space symmetry (Γ_{rh} C_43 , space group number 146). In *R3* space symmetry there is only one 3-fold rotational axis (say, [1, 1, 1] in terms of cubic system) and there are only two different channels for the $P2_13$ (Γ_c T_4) → *R3* (Γ_{rh} C_43) symmetry lowering. The first involves the quadrupole active mode at the X point [$q_X = \pi/a(1, 0, 0)$] of the Brillouin zone, while the second is connected with the quadrupole mode at the R point [$q_R = \pi/a(1, 1, 1)$] of the Brillouin zone. Which mode actually drives the transformation depends on the energy lowering associated with the mode and requires an additional study. Both modes (X and R) are considered in detail in Appendix.

From the performed analysis, Appendix, it follows that the structural phase transitions would be of the second order if the Lifshitz condition had been fulfilled. In our case the Lifshitz condition is violated and for both cases (q_X and q_R modes) the Lifshitz frequency is not zero. This implies that in the expansion of the Landau free energy in order parameter components ηi, antisymmetrical contributions of the type $\eta_k\eta'_i - \eta_i\eta'_k$ etc. are not zero. Such contributions make the phase transition incommensurate (or modulated) and we attribute it to the anomalous behavior of CoGe at T ≈ 13 – 14 K. The low temperature phase (at temperatures $T < T_c$ = 14 K) then can be incommensurate with the wave vector ≈ q lying close to q_X or q_R. In conclusion, both discussed schemes of the $P2_13$ (Γ_c T_4) → *R3* (Γ_{rh} C_43) symmetry lowering considered in Appendix indicate that it is a commensurate-incommensurate phase transition.

The transition from commensurate to incommensurate phase will lead to a weak anomaly in the measured heat capacity compared to the second-order phase transition, since the transformation due to the gradient contribution to the free energy is smoother.